Stanford Exploration Project, Report 120, May 3, 2005, pages 167–179

Non-linear estimation of vertical delays with a quasi-Newton method

Antoine Guitton, Jesse Lomask, and Sergey Fomel[1]

ABSTRACT

A local dip (or step out) between two adjacent traces embeds the necessary information to go from one reflection on one trace to the same reflection on the next. In more dimensions, i.e., 3-D, the same result is obtained between distant traces by integrating the local dips in all directions, thus obtaining relative delay maps useful for (1) automatic full-volume picking and (2) automatic flattening of horizons. The estimation of these maps from local dips is a non-linear process. In this paper, this problem is solved with a quasi-Newton technique for 2-D slices and 3-D cubes. Furthermore, the estimation of the relative delays is done globally in a least-squares sense for all reflectors at once. Synthetic and field data examples illustrate the ability of the algorithm to flatten horizon according to their geological time. As a natural extension of our algorithm, any horizon can also be picked automatically at no additional cost.

INTRODUCTION

From the estimation of local dips, Lomask (2003a) showed that vertical shifts (time or depth) can be estimated to flatten seismic data in 2-D or 3-D. The basic idea is to integrate local dips or step outs estimated from the data. This integration gives for every point in the data volume a relative vertical (time or depth) delay to one event present on a reference trace. This delay can be used for flattening, where each sample is shifted according to the delay value, or for picking, where one event (or many events) can be followed from the reference trace to everywhere in the data volume by simply stepping up or down according to the delay value. In addition, time/depth shift estimation can be used for many geophysical applications. For instance, Wolf et al. (2004) illustrate how RMS velocities can be estimated without picking. Similarly, Guitton et al. (2004) solve a tomographic problem by inverting the time delays.

Lomask (2003b) identified a non-linear relationship between the local dips and the relative delays. In his approach, however, this property was first ignored by solving simpler linear problems. The goal of this paper is to solve the non-linear problem exactly with a quasi-Newton approach called L-BFGS (Guitton and Symes, 2003). Solving the non-linear problem allows us to estimate relative time/depth shifts when the local dips are not constant with time or depth, a central assumption in the linear approach of Lomask (2003a).

[1]**email:** antoine@sep.stanford.edu, lomask@sep.stanford.edu, sergey.fomel@beg.utexas.edu

This paper starts with a presentation of the theory of time/depth delay estimation in 2-D and 3-D. The quasi-Newton method is briefly introduced. Then, the proposed algorithm is tested on 2-D and 3-D data examples. They illustrate the accuracy of the method to compute relative time/depth delays and to perform event picking.

THEORY OF TIME/DEPTH DELAYS ESTIMATION

First consider a data volume $d(x,y,z)$ where x and y are the horizontal axes and z is the depth or time axis. Building on Lomask (2003b), a vertical (time or depth) delay function $\tau(x,y,z)$ is estimated by minimizing the following functional $J(\tau)$:

$$J(\tau) = \int\int \left[\left(p_x(x,y,z;\tau) - \frac{\partial \tau}{\partial x} \right)^2 + \left(p_y(x,y,z;\tau) - \frac{\partial \tau}{\partial y} \right)^2 \right] dx\, dy, \tag{1}$$

where p_x is the local step-out vector estimated in the x direction and p_y is the local step-out vector estimated in the y direction. Both vectors depend on τ, which makes the problem of finding the time/depth delays non-linear.

In this paper, we propose solving for $\tau(x,y,z)$ with a quasi-Newton method called L-BFGS (Guitton and Symes, 2003). The quasi-Newton method is an iterative process where the solution to the problem is updated as follows:

$$\tau_{k+1} = \tau_k - \lambda_k \mathbf{H}_k^{-1} \nabla J(\tau_k), \tag{2}$$

where τ_{k+1} is the updated solution at iteration $k+1$, λ_k the step length computed by a line search that ensures a sufficient decrease of $J(\tau)$ and $\mathbf{H}_k$ an approximation of the Hessian (or second derivative.) One important property of L-BFGS is that it requires the gradient of $J(\tau)$ only to build the Hessian. The gradient $\nabla J(\tau)$ of $J(\tau)$ can be found by introducing the Euler-Lagrange equation and is given by:

$$\nabla J(\tau) = -\frac{\partial^2 \tau}{\partial x^2} - \frac{\partial^2 \tau}{\partial y^2} + \frac{\partial p_x}{\partial x} + \frac{\partial p_y}{\partial y} + \frac{1}{2}\frac{\partial {p_x}^2}{\partial \tau} + \frac{1}{2}\frac{\partial {p_y}^2}{\partial \tau} \tag{3}$$

The 2-D case is a simple extension of this result where the terms in y are dropped. In practice, the last four terms of the gradient in equation (3) can be precomputed and evaluated at $\tau_k(x,y,z)$ when needed for the BFGS update. This saves a lot of computational effort. Note that the relative vertical (time or depth) delays are computed with respect to a reference trace chosen a priori in the data volume. A weight that would throw-out fitting equations at fault locations can also be incorporated easily in both the gradient and objective function.

The most important components of this time/depth delay evaluation technique are the dip fields p_x and p_y. In our implementation, we use the method of Fomel (2002) to estimate both. This technique estimates local dips from adjacent traces without slant-stacking. It also gives one dip value only for each data point. Next, 2-D and 3-D data examples illustrate the flattening technique.

2-D DATA EXAMPLES

The 2-D algorithm, a simple extension of the 3-D algorithm, is illustrated first on five synthetic (Figures 1 to 5) and one field data examples (Figure 6). All these figures are organized as follows: panel (a) shows the input data, panel (b) shows the estimated dip field using Fomel's technique (Fomel, 2002), (d) shows the picking result where the seed point starts from the reference trace every ten samples in time/depth, and (d) shows the flattening result. The field data example is a 2-D slice extracted from the Elf (now Total) L7D dataset after common-azimuth depth migration (Vaillant et al., 2000). All these examples illustrate that the time/depth delay estimation process is very accurate and robust.

3-D DATA EXAMPLES

The 3-D algorithm is tested on two datasets from the Gulf of Mexico. Figures 7a, 7b, and 7c show the input data, the picked reflector, and the flattening result for the first dataset. The size of this dataset is 100x100x100 samples. After flattening in Figure 7c, a channel is now clearly visible. Note that the picked reflectors in Figure 7b follow extremely well the true reflectors. Again, this result is obtained at no cost and is readily available from the estimation of $\tau(x, y, z)$.

Figures 8a, 8b, and 8c show the input data, the picked reflector, and the flattening result for the second dataset. The size of this dataset is 200x200x200 samples. It features more complicated structures such as a large salt body on the left (shown as SF) and faults. Nothing was done to pick the faults, as suggested by (Lomask et al., 2005). Nevertheless, the flattening result in Figure 8c highlights one channel on the depth slice that was not previously visible. The picking result in Figure 8b is also very accurate.

CONCLUSION

Estimating time/depth delays from dip fields is a non-linear problem. A quasi-Newton technique was introduced to solve it. Several 2-D and 3-D examples illustrate the efficiency of this method to flatten and automatically interpret seismic horizons without any picking.

ACKNOWLEDGEMENTS

We thank ChevronTexaco for providing the dataset used in the first 3-D example, and Joe Reilly at ExxonMobil for the second 3-D dataset.

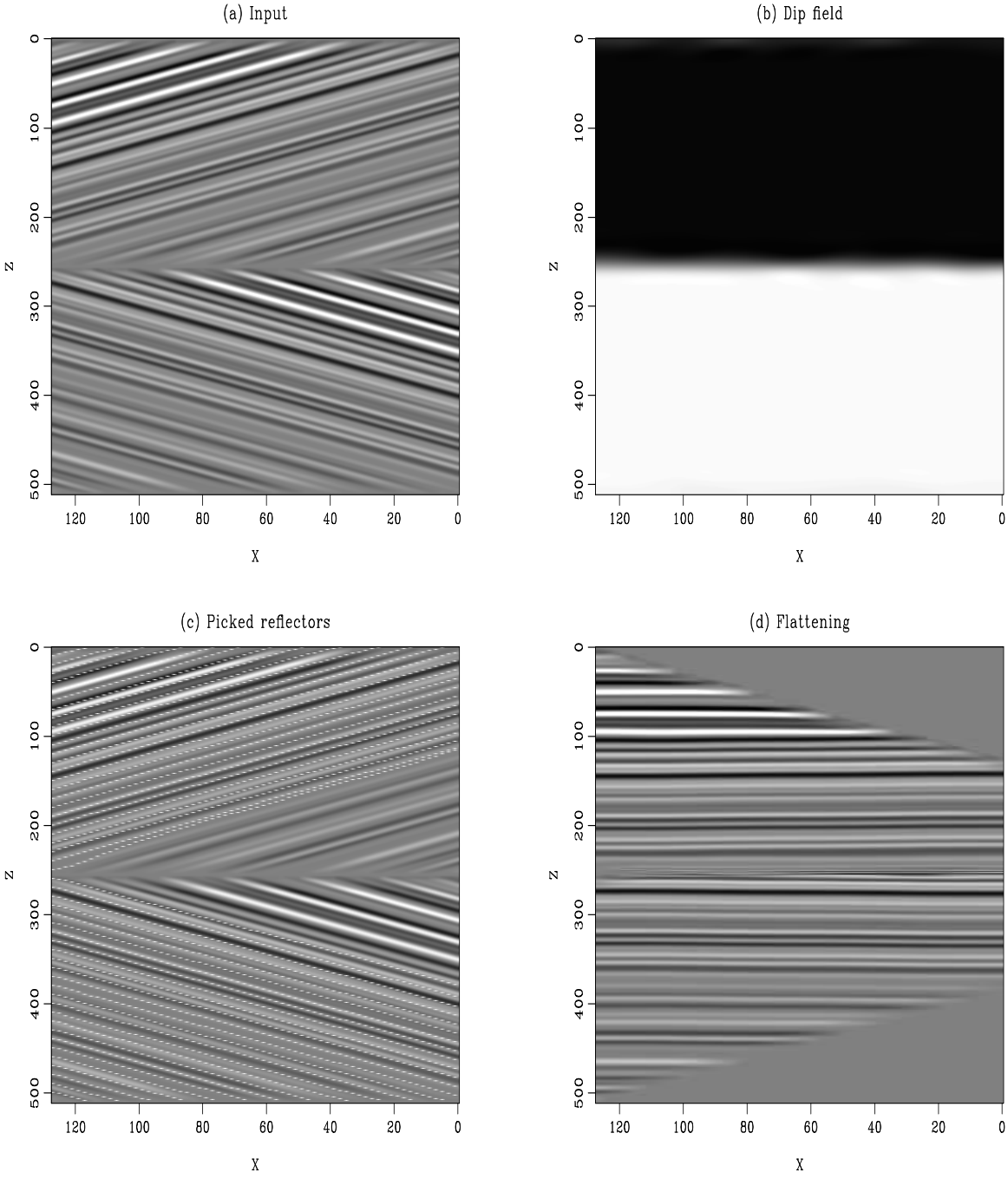

Figure 1: (a) Model. (b) Estimated dips. (c) Automatic picking of few horizons. (d) Flattening result. The first trace is used for reference. antoine1-unconformity [ER]

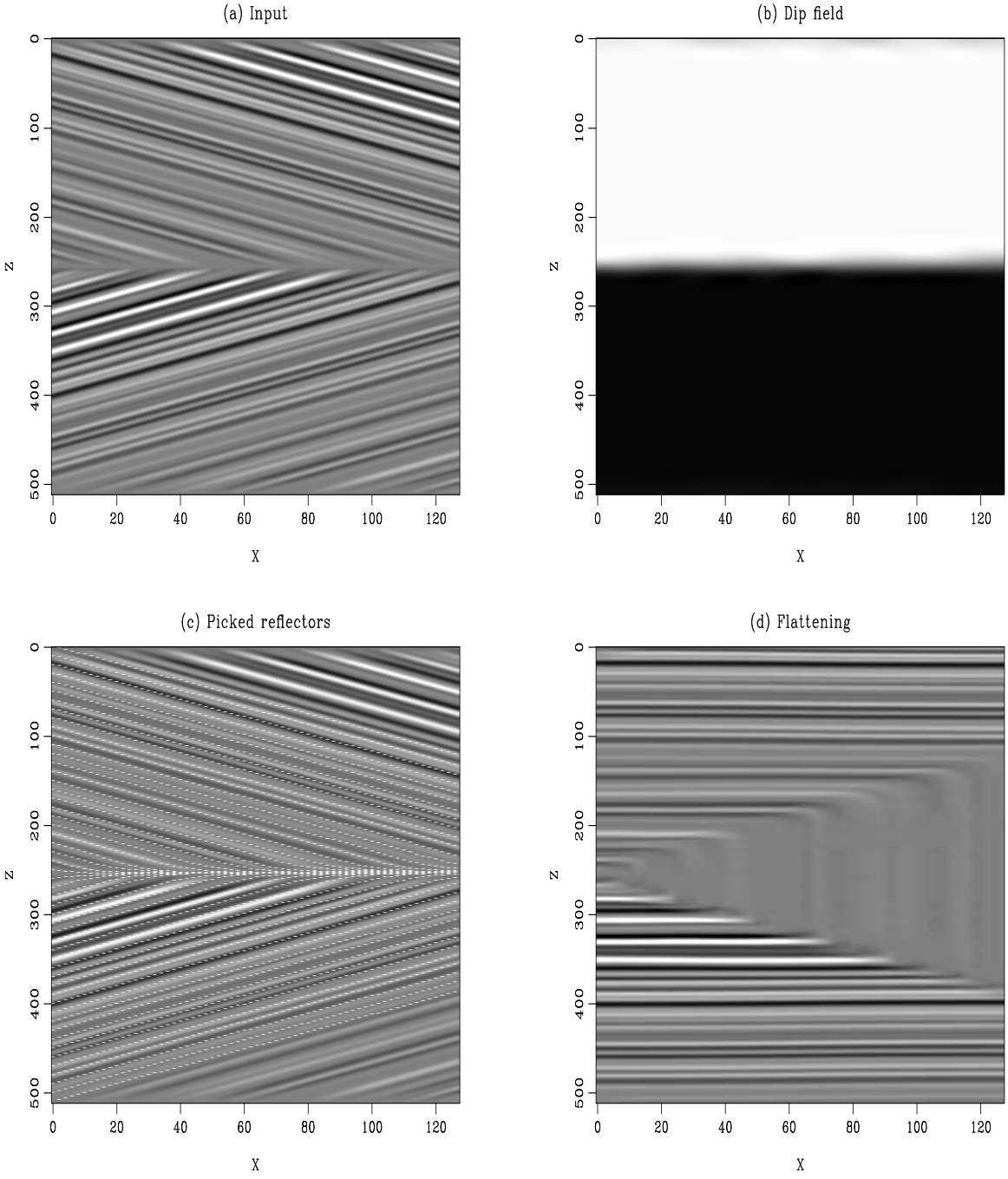

Figure 2: (a) Model. (b) Estimated dips. (c) Automatic picking of few horizons. (d) Flattening result. The first trace is used for reference. antoine1-unconformity2 [ER]

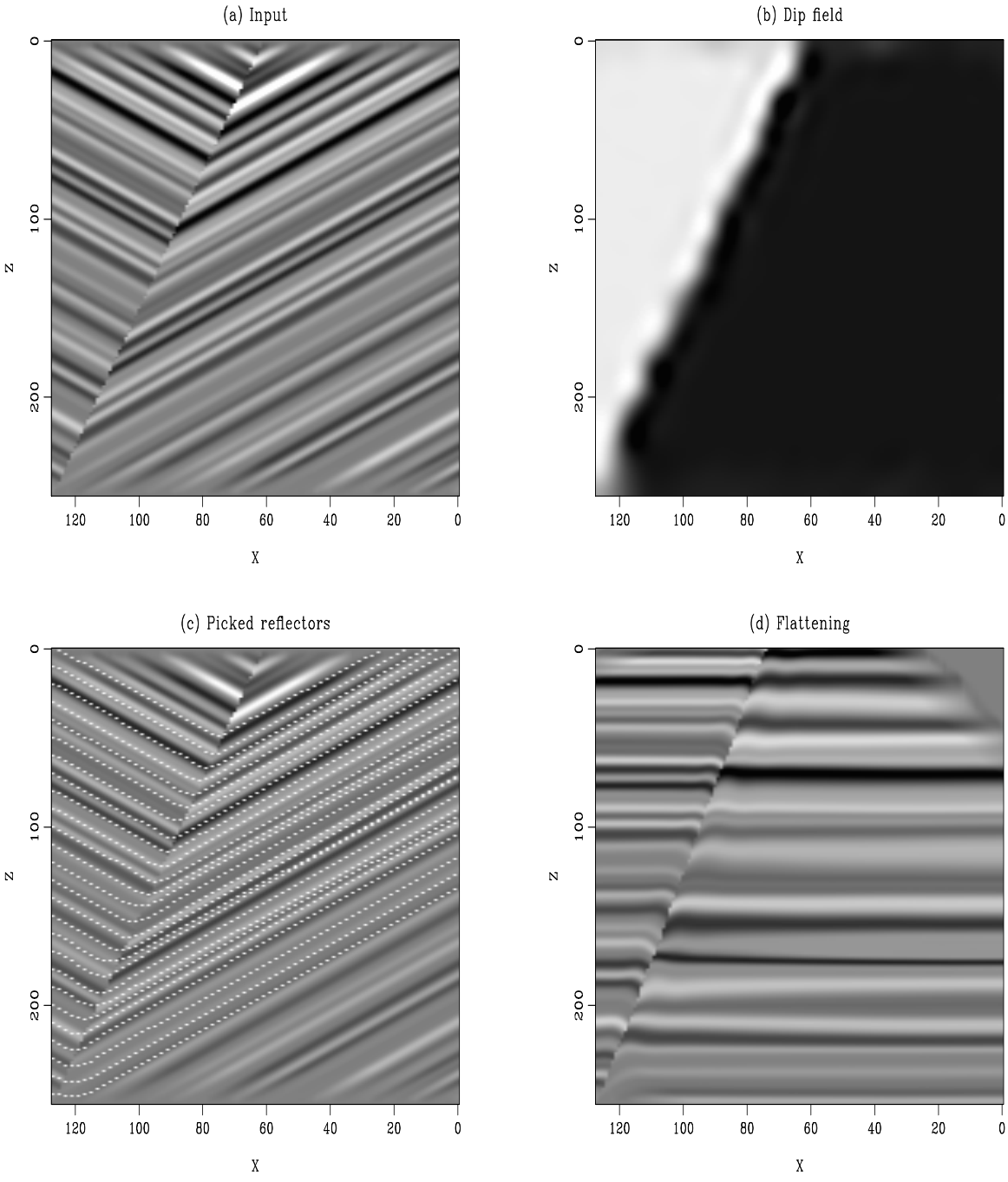

Figure 3: (a) Model. (b) Estimated dips. (c) Automatic picking of few horizons. (d) Flattening result. The smoothness of the estimated dips introduce small errors in the flattening result. The first trace is used for reference. antoine1-unconformity3 [ER]

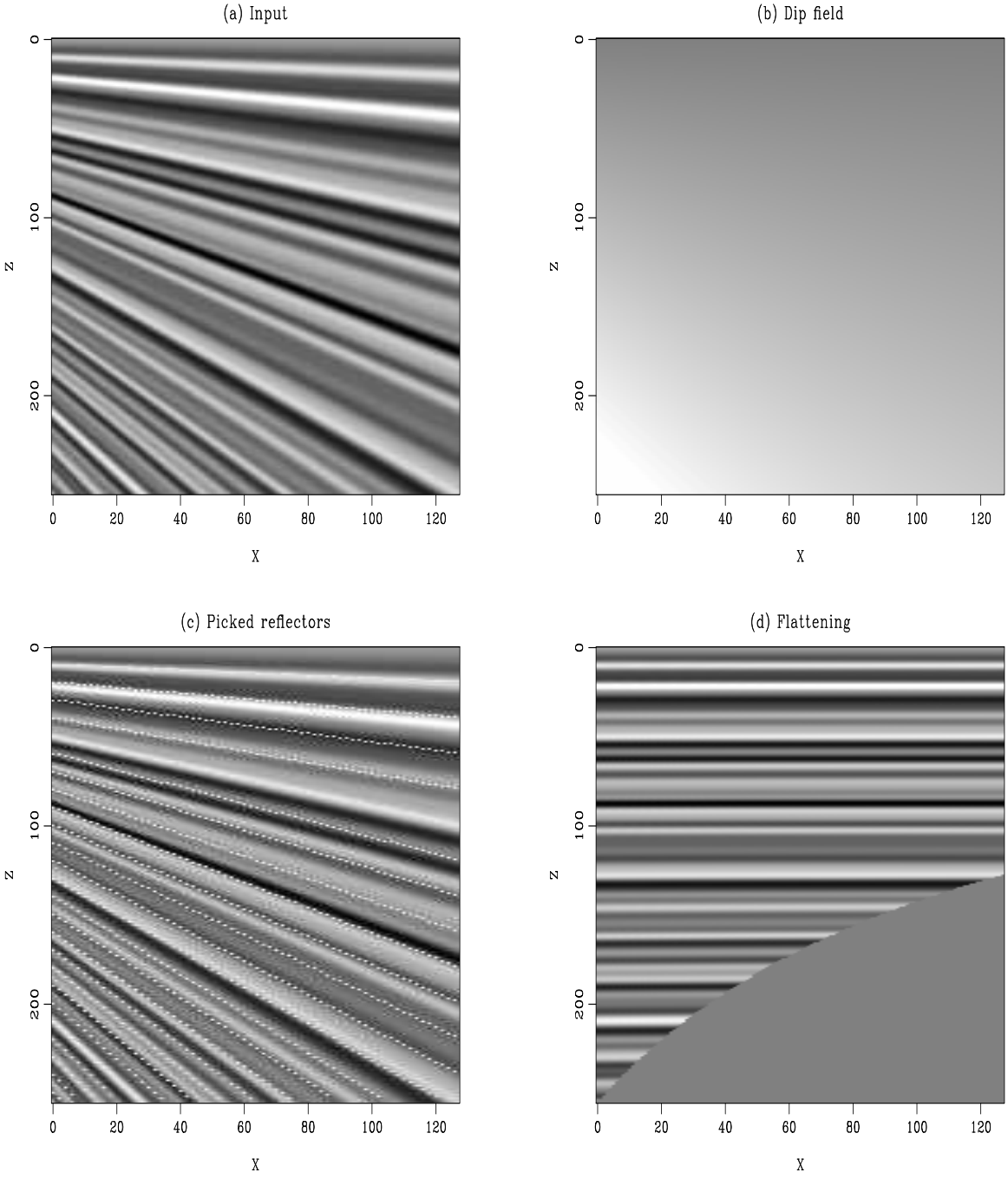

Figure 4: (a) Model. (b) Estimated dips. (c) Automatic picking of few horizons. (d) Flattening result. The first trace is used for reference. antoine1-thinning3 [ER]

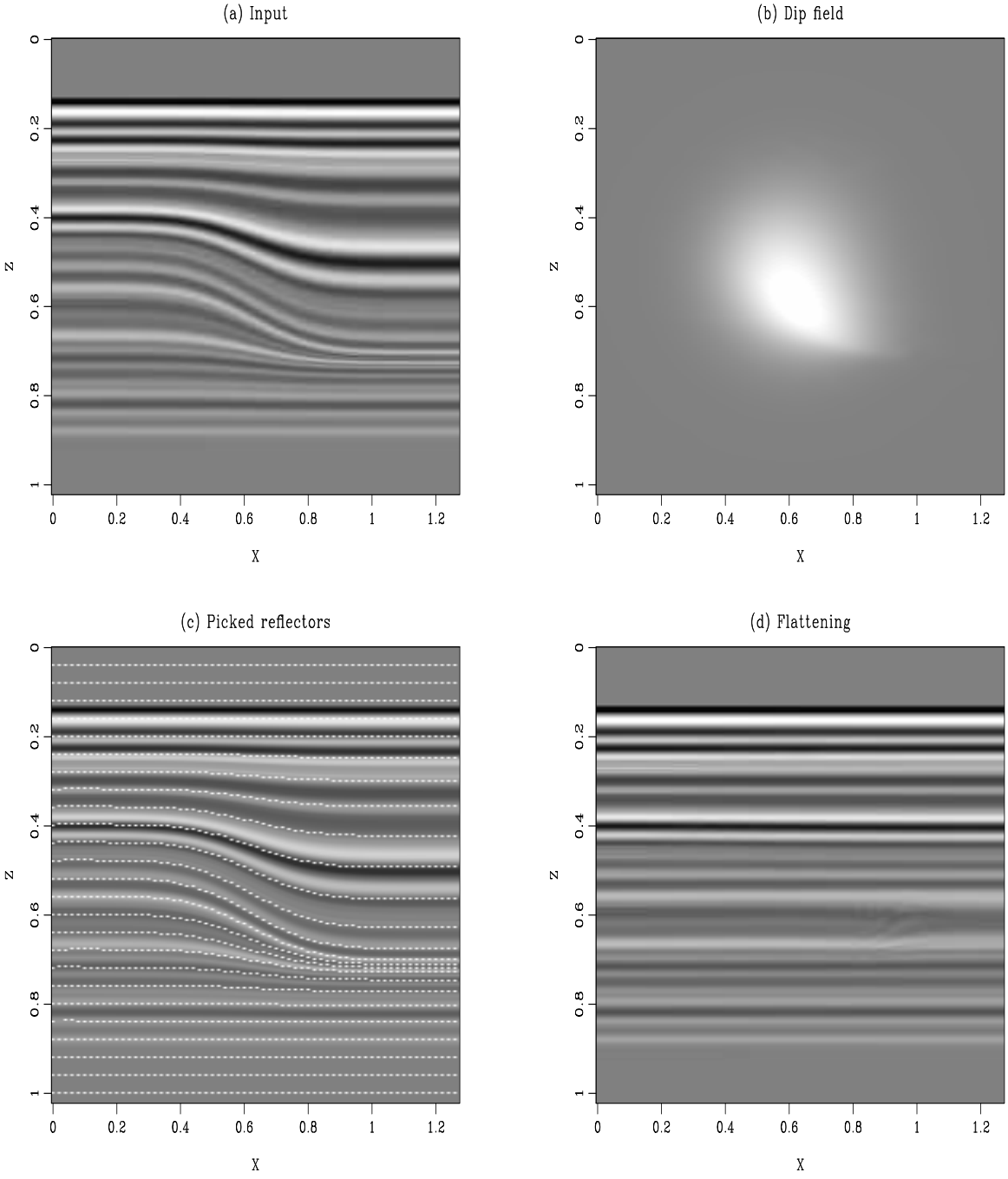

Figure 5: (a) Model. (b) Estimated dips. (c) Automatic picking of few horizons. (d) Flattening result. The first trace is used for reference. antoine1-down_lap2D [ER]

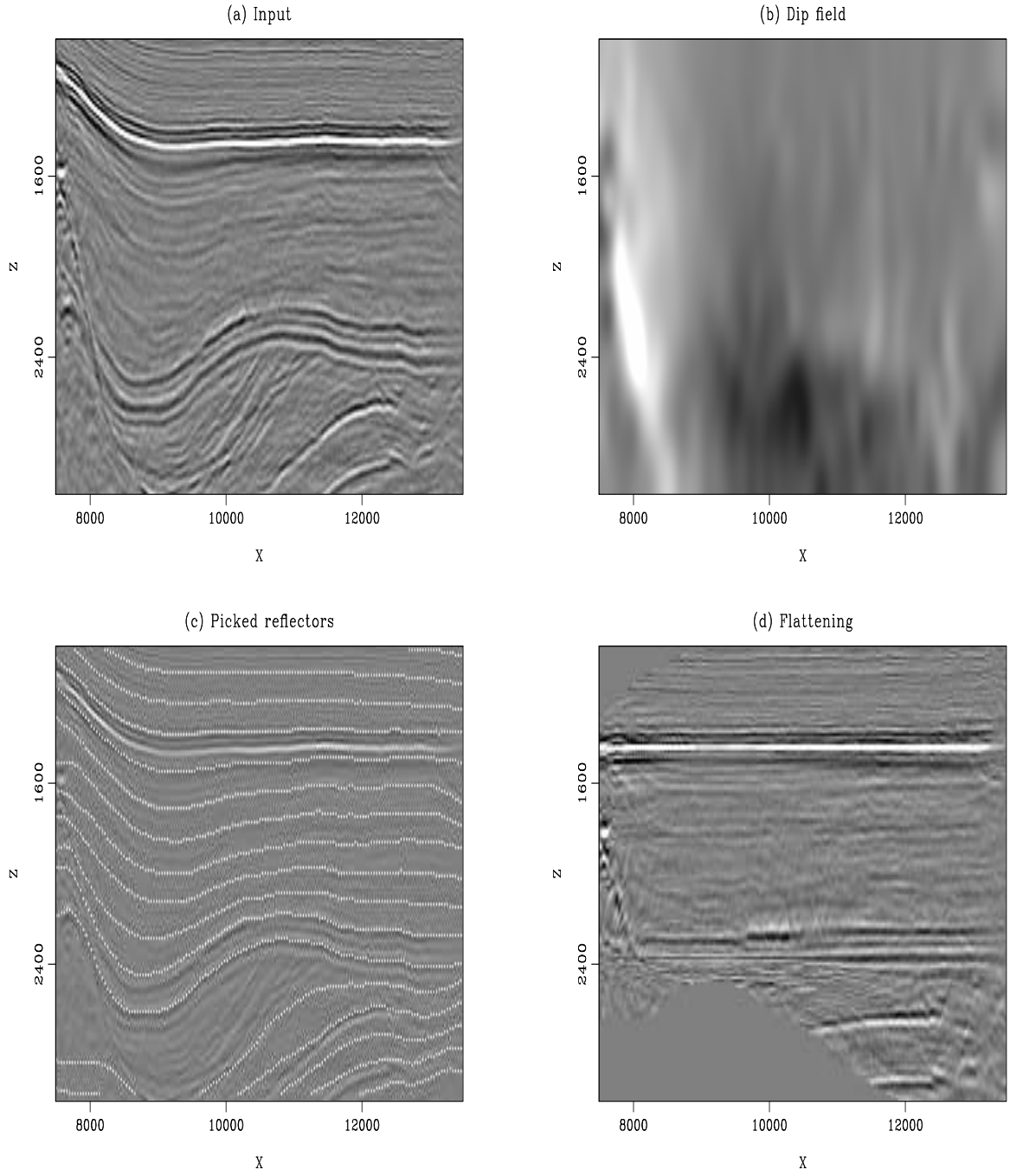

Figure 6: (a) Model. (b) Estimated dips. (c) Automatic picking of few horizons. (d) Flattening result. The picked horizons follow extremely well the structure of the data. The trace at X=12000 is used for reference. antoine1-elf2D [ER]

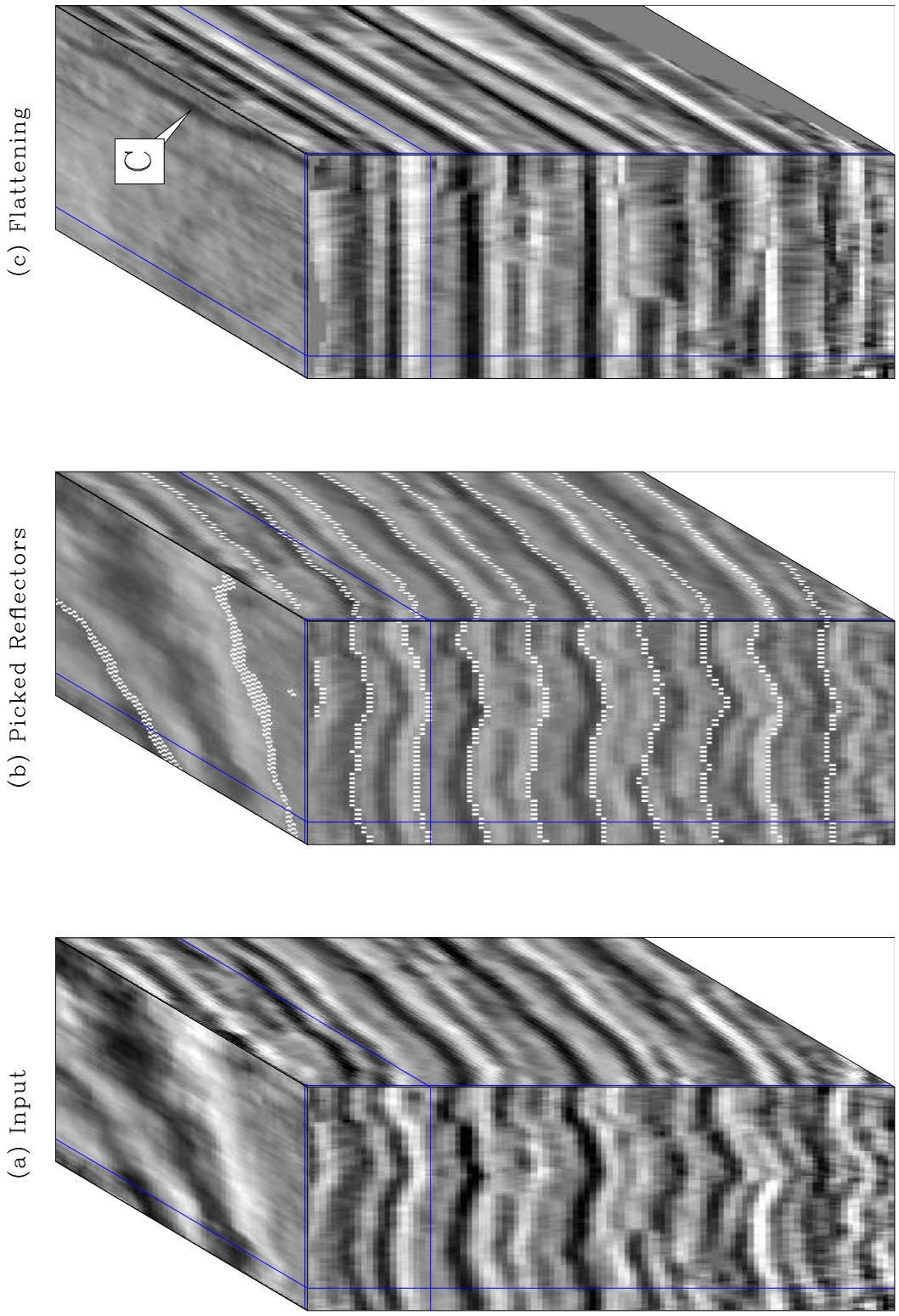

Figure 7: (a) Model. (b) Automatic picking of few horizons. (c) Flattening result. The picked horizons follow extremely well the structure of the data. On the time slice (top panel) a channel (marked as C), previously unseen in the data, is revealed by the flattening process. antoine1-3D-data-shoal-test [CR]

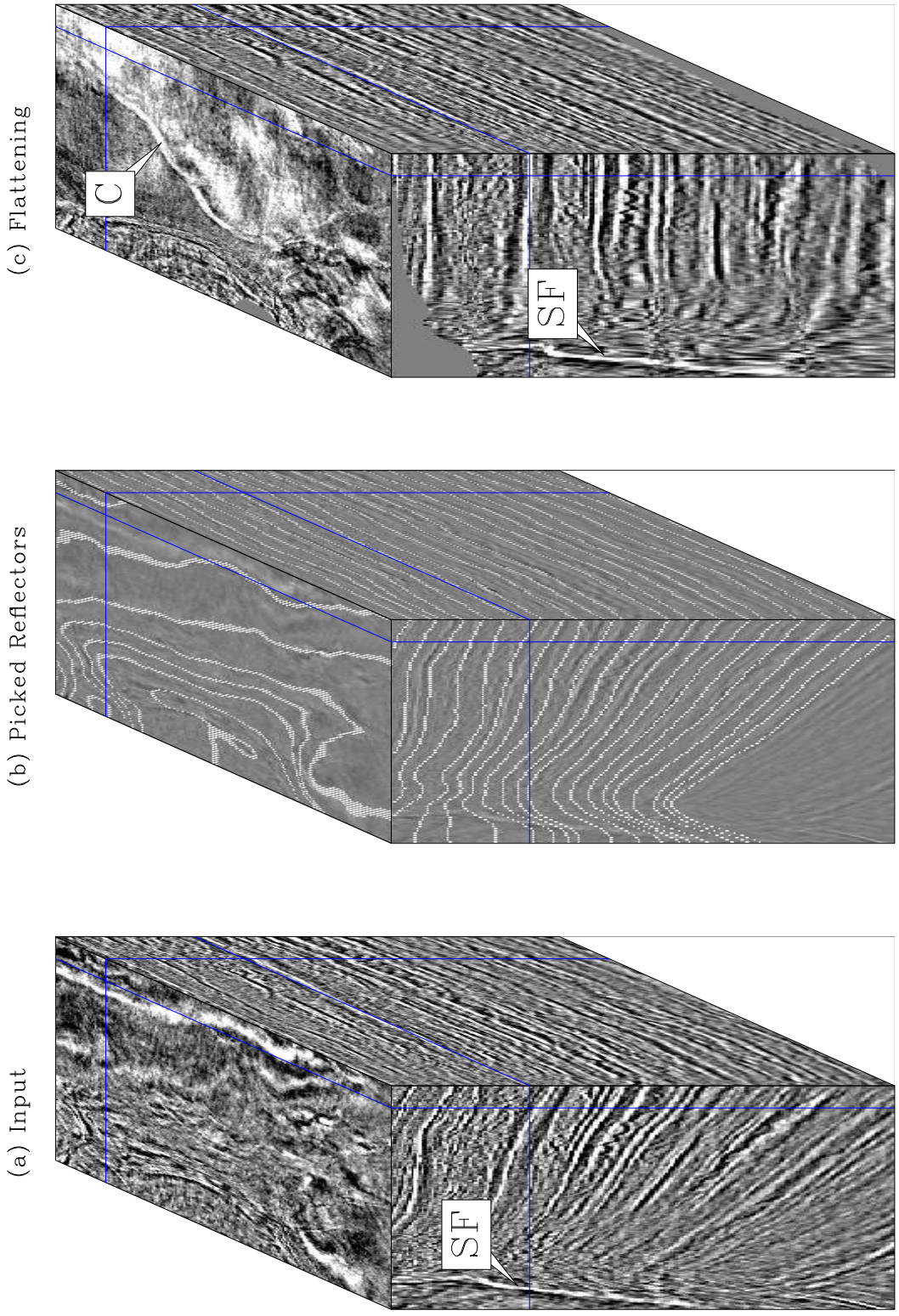

Figure 8: (a) Model. (b) Automatic picking of few horizons. (c) Flattening result. On the depth slice (top panel) a channel (marked as C), previously unseen in the data, is revealed by the flattening process. Arrow SF shows the salt flanks. antoine1-3D-ExxonMobil-data [CR]

REFERENCES

Fomel, S., 2002, Applications of plane-wave destruction filters: Geophysics, **67**, no. 06, 1946–1960.

Guitton, A., and Symes, W., 2003, Robust inversion of seismic data using the Huber norm: Geophysics, **68**, no. 4, 1310–1319.

Guitton, A., Claerbout, J., and Lomask, J., 2004, First-order lateral interval velocity estimates without picking:, *in* 74th Ann. Internat. Mtg. Soc. of Expl. Geophys., 2339–2342.

Lomask, J., Guitton, A., and Valenciano, A., 2005, Flattening without picking faults: SEP–**120**, 159–166.

Lomask, J., 2003a, Flattening 3D seismic cubes without picking: Soc. of Expl. Geophys., 73rd Ann. Internat. Mtg., 1402–1405.

Lomask, J., 2003b, Flattening 3-D data cubes in complex geology: SEP–**113**, 247–260.

Vaillant, L., Calandra, H., Sava, P., and Biondi, B., 2000, 3-D wave-equation imaging of a North Sea dataset: Common-azimuth migration + residual migration: Soc. of Expl. Geophys., 70th Ann. Internat. Mtg, 874–877.

Wolf, K., Rosales, D. A., Guitton, A., and Claerbout, J., 2004, Robust moveout without velocity picking:, *in* 74th Ann. Internat. Mtg. Soc. of Expl. Geophys., 2423–2426.